JPEDAV (2008) 29:101–109
DOI: 10.1007/s11669-007-9017-x
1547-7037 ©ASM International

The Ga-Mn-Ni (Gallium-Manganese-Nickel) System

K. P. Gupta , The Indian Institute of Metals

The Ga-Mn-Ni system has attracted a lot of attention due to shape memory found for a Heusler-type $GaMnNi_2$ alloy that is also ferromagnetic. However, very little work has been done on phase equilibria of the ternary system. The available information on the Ga-Mn-Ni system is reported here.

Binary Systems

The Ga-Mn system [Massalski2] (Fig. 1[†]) has eight intermediate phases, ω ($Ga_{4.6}Mn$), ϕ ($Ga_{3.3}Mn$), ι ($Ga_{2.3}Mn$), η ($GaMn_{1.2}$ (LT)), λ ($GaMn_{1.2}$ (HT)), γ_2 ($GaMn_{1.7}$), γ_3 ($GaMn_{1.4}$), and ε_1 ($GaMn_{2.5}$). Except for the ε_1 phase, which forms congruently from the face-centered cubic (fcc) γ phase at 820 °C, all the other phases form through peritectic or peritectoid reactions: $L + \delta Mn \leftrightarrow \lambda$ at 830 °C, $\lambda + \gamma_3 \leftrightarrow \eta$ at 600 °C, $L + \eta \leftrightarrow \phi$ at 520 °C, and $L + \phi \leftrightarrow \omega$ at 410 °C. Several eutectic-type or eutectoid reactions occur in the Ga-Mn system: $L \leftrightarrow (Ga) + \omega$ at ≤29.8 °C, $\lambda \leftrightarrow L + \eta$ at 520 °C, $(\delta Mn) \leftrightarrow \lambda + \gamma_3$ at 715 °C, and $\gamma_3 \leftrightarrow \varepsilon_1 + (\beta Mn)$ at 620 °C. The (βMn) phase exists from ~80 to 100 at.% Mn at the higher temperatures, but at or below 727 °C the αMn phase exists. The γ_3, γ_2, and γ phase boundaries are not well determined. γ is the fcc terminal solid solution (γMn).

The Ga-Ni system [1991Nas] (Fig. 2) has eight intermediate phases, β_1 (Ni_3Ga), δ'(Ni_5Ga_3), ε(Ni_3Ga_2(HT)), γ' (Ni_3Ga_2 (LT)), ν (GaNi), θ (Ga_4N_3), β_2 (Ga_3Ni_2), and ρ (Ga_4Ni), of which the ν phase melts congruently at 1220 °C. The β_1, β_2, ρ, and (Ga) phases form through peritectic reactions: $\gamma + L \leftrightarrow \beta_1$ at 1212 °C, $L + \nu \leftrightarrow \beta_2$ at 895 °C, $L + \beta_2 \leftrightarrow \rho$ at 363 °C, and $L + \rho \leftrightarrow$ (Ga) at 30.2 °C; the ε, δ', and θ phases form through peritectoid reactions: $\beta_1 + \nu \leftrightarrow \varepsilon$ at 949 °C, $\beta_1 + \varepsilon \leftrightarrow \delta'$ at 741 °C, and $\nu + \beta_2 \leftrightarrow \theta$ at 542 °C. The $\varepsilon \leftrightarrow \gamma'$ phase transformation occurs at ~680 °C. A eutectic reaction $L \leftrightarrow \beta_1 + \nu$ occurs at 1207 °C.

The Mn-Ni system [Massalski2] (Fig. 3) is a single peritectic system with the peritectic reaction $L + (\delta Mn) \leftrightarrow \gamma$ occurring at 1164 °C and has a liquidus/solidus minimum of 1020 °C occurring at ~38 at.% Ni. The γMn and Ni form a continuous solid-solution phase γ. The γ phase transforms to the ν (MnNi (HT)), ξ (Mn_2Ni (HT)), and ζ ($MnNi_2$ (HT)) phases congruently at 911, 720, and 710 °C, respectively. Several other intermediate phases, ζ' ($MnNi_2$ (LT)), η_1 (MnNi (MT)), η_2 (MnNi (LT)), γ_1 ($MnNi_3$), and κ (Mn_3Ni) phases, form through peritectoid reactions: $\gamma + \nu \leftrightarrow \eta_1$ at 775 °C, $\eta_2 + \gamma_1 \leftrightarrow \zeta'$ at 440 °C, $(\alpha Mn) + \gamma \leftrightarrow \gamma_1$ at 520 °C, $(\alpha Mn) + \gamma_1 \leftrightarrow \eta_2$ at 480 °C, and $(\alpha Mn) + \eta_2 \leftrightarrow \kappa$ at 430 °C. Several eutectoid reactions take place: $\nu \leftrightarrow \gamma + \eta_1$ at 675 °C, $\eta_1 \leftrightarrow \xi + \zeta$ at 620 °C, $\zeta \leftrightarrow \xi + \gamma$ at 580 °C, $\xi \leftrightarrow (\alpha Mn) + \gamma$ at 560 °C, $\gamma \leftrightarrow \eta_1 + \zeta$ at 655 °C, $\gamma \leftrightarrow \xi + \eta_1$ at 640 °C, $\gamma \leftrightarrow (\beta Mn) + \xi$ at 615 °C, and $(\beta Mn) \leftrightarrow (\alpha Mn) + \xi$ at 586 °C.

Binary and Ternary Phases

In the three binary systems Ga-Mn, Ga-Ni, and Mn-Ni, 24 intermediate phases form. No ternary intermediate phase has been reported in the Ga-Mn-Ni system except that an ordered $GaMnNi_2$ phase forms in a certain composition region of the extended ν phase region that exists between the GaNi and the MnNi phases. The phases and their structure data are given in Table 1.

Ternary System

The existence of a $GaMnNi_2$ phase was first reported by [1960Ham], who made exploratory work on Heusler-type (Structurbericht-type $L2_1$ structure) $AMnB_2$ alloys, where A = Ga, In, or Sb and B = Co, Ni, or Pd. The $GaMnNi_2$ phase was found both in alloys quenched from 940 °C and in furnace-cooled alloys. Since Ni and Mn have very closely comparable scattering factors the phase was tentatively identified by x-ray diffraction as the $AlMnCu_2$ type ($L2_1$) structure. The $GaMnNi_2$ alloy was found to be ferromagnetic. [1968Web] used a powder neutron diffraction at room temperature and confirmed that the $GaMnNi_2$ alloy has the $L2_1$ type structure. The alloy, however, showed a transformation at liquid N_2 temperature. Further, higher-resolution neutron diffraction work by [1984Web] at room temperature and at liquid He temperature, by both rocking crystal neutron diffraction and optical microscopy, showed that the transformation at low temperature is a martensitic type with $M_s \approx 71$ °C (202 K) and is completely reversible. The diffraction pattern suggested the martensitic phase to be of tetragonal symmetry with lattice parameter $a = 0.592$ nm, $c = 0.5566$ nm, and $c/a = 0.94$. Rocking crystal neutron [1984Web] and x-ray [1990Zas] diffraction patterns showed major diffraction peaks with weak diffraction peaks. It was deduced from the weak diffraction peaks that they arise due to periodic displacement of (110) planes along the $[1\bar{1}0]$ direction, the

K. P. Gupta, The Indian Institute of Metals, Calcutta, India; Contact e-mail: iiom@cal2.vsnl.net.in

[†]Note, that the diagram in Fig. 1 shows no two phase region between the single-phase region of the γ, γ_2, and γ_3 region. This implies higher order transitions. However, available data is not conclusive at this point.

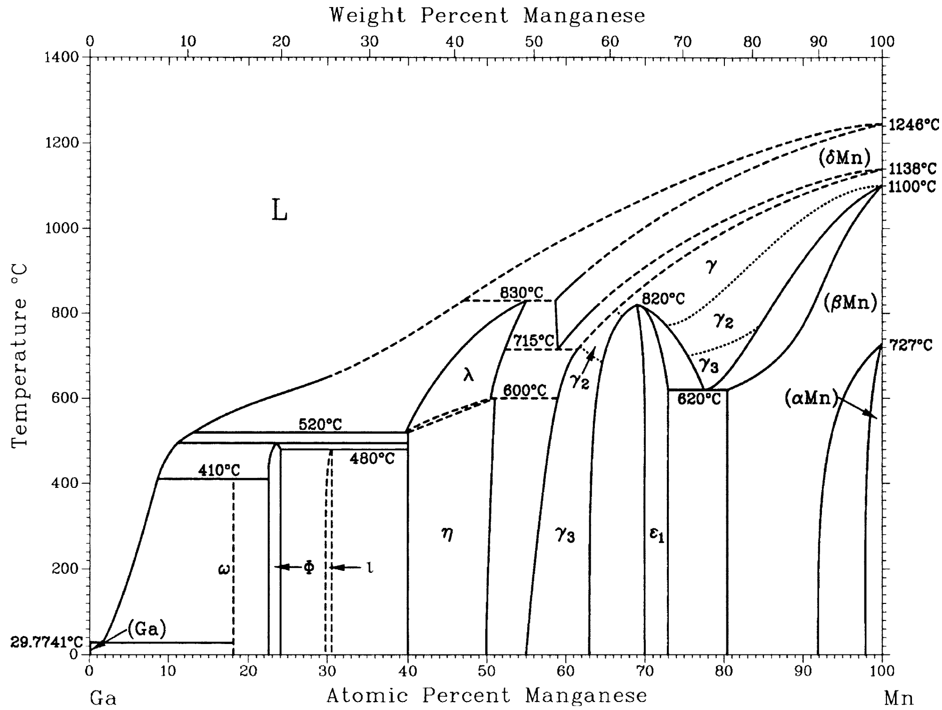

Fig. 1 Binary Ga-Mn system [Massalski2]

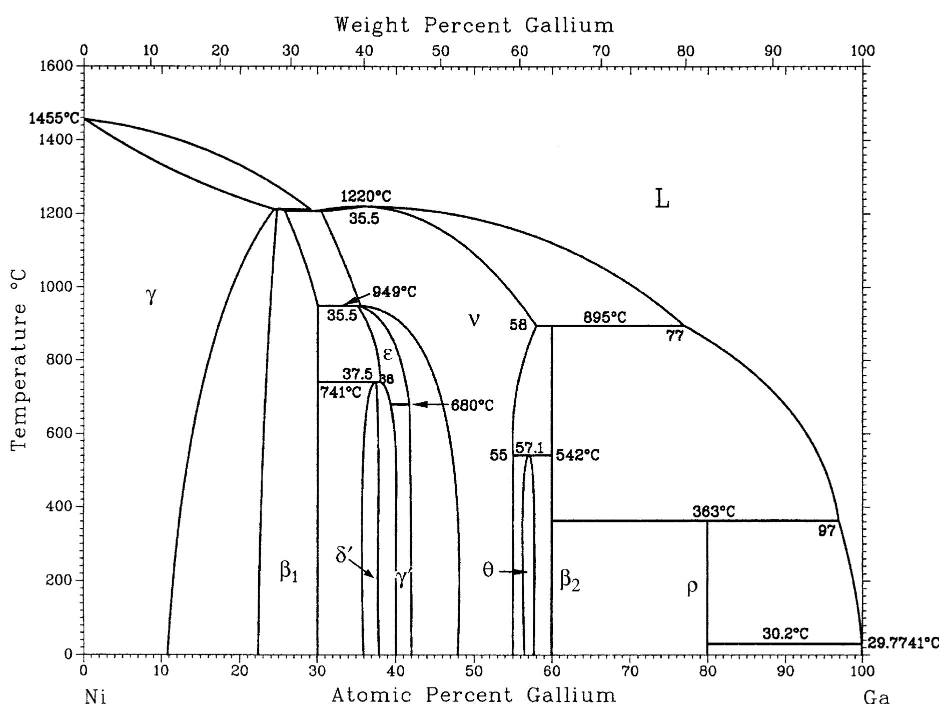

Fig. 2 Binary Ga-Ni system [1991Nas]

periodicity being ~5. Using electron diffraction patterns [1999Wed] confirmed the periodicity to be 5, but on quenching the specimen to below 173 K (−100 °C) the periodicity increased to 7, and on warming the specimen the periodicity reverted back to 5. The low-temperature crystal structure of the martensite was found to be of tetragonal structure, but unlike [1984Web] the lattice parameter was found to be a = 0.3877 nm, c = 0.6489 nm, a superstructure cell based on AuCu-type cell with doubled c axis.

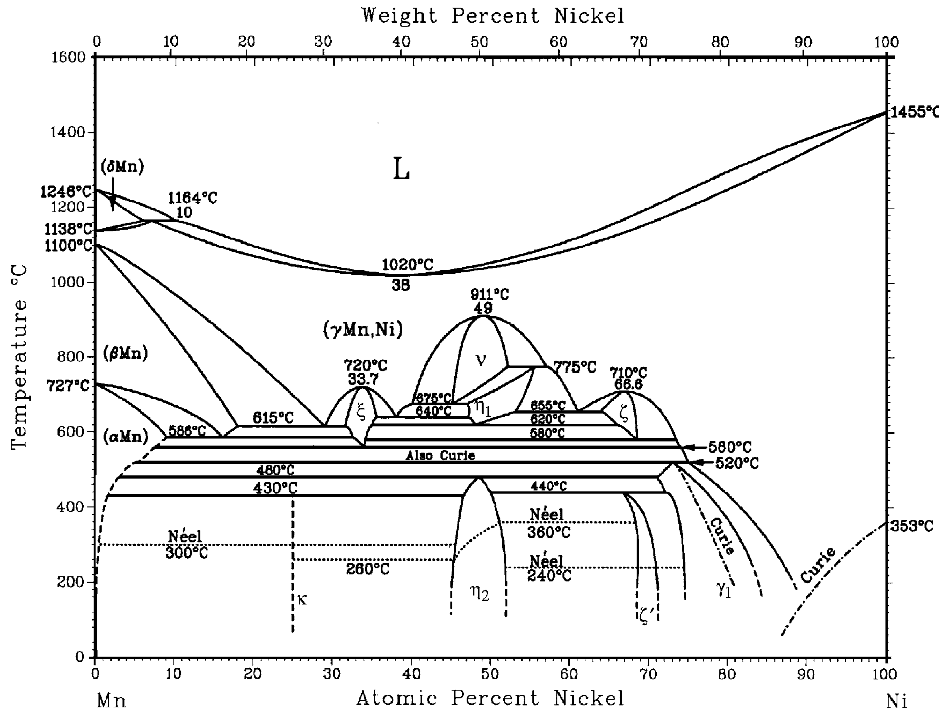

Fig. 3 Binary Mn-Ni system [Massalski2]

Compression testing of $GaMnNi_2$ single crystals along the $\langle 100 \rangle$ direction induced a martensitic transformation in the crystals [1990Zas], and the stress required to initiate martensitic transformation was found to increase linearly with temperature. The modulus of elasticity of the initial state of a $GaMnNi_2$ alloy was found to be $E_{\langle 100 \rangle} = (5 \pm 2) \times 10^9$ GPa. Heat capacity of a $GaMnNi_2$ alloy measured with a differential scanning calorimeter showed two thermal effects, one at ~280 K (~3 °C) that is related to the phase transformation and a λ -type thermal effect related to ferromagnetic to paramagnetic transformation; the Curie temperature T_C was ~370 K (97 °C). The entropy change ΔS due to the phase transformation was estimated to be 3.1 J/mol·K. [1996Che] used hydrostatic pressure to initiate martensitic transformation in $GaMnNi_2$ single crystal and observed a linear increase in martensite start temperature M_s with pressure up to ~1.2 GPa (Fig. 4).

The variation of physical properties and structural transformation temperature with composition of the ν phase around the $GaMnNi_2$ alloy composition was studied in a limited way by [1997Wir] and somewhat more extensively by [1995Che]. [1995Che] used alloys in the composition region of 25-30 at.% Ga, 20-30 at.% Mn, and 45-55 at.% Ni and determined M_s, thermal hysteresis of transformation (ΔT), transformation heat (Q), and Curie temperature (T_C). For these alloys ΔT varied from ~7 ° to ~30 °C, Q varied from 1.3 to 11.0 J/g, T_C varied from 308 ° to 387 K (35-114 °C), but M_s was found to vary over wide temperature range, from <4.2 to 626 K (< −269 ° to 353 °C). The variation of M_s as a function of Ga and Mn content at approximately constant third-element content of the alloys is given in Fig. 5, and the following conclusions have been drawn:

- At constant value of Mn content, Ga addition lowers M_s.
- Mn additions (instead of Ga) at constant Ni causes M_s to rise.
- Substitution of Ni by Mn at constant Ga content lowers M_s.

No reason for the wide variation of M_s with composition has been given.

Very little work has been done to establish phase equilibria in the Ga-Mn-Ni system. Both GaNi and MnNi phases have the same crystal structure (CsCl ($B2$) type), and they are expected to form at some elevated temperature a continuous phase region ν from which the $GaMnNi_2$ type-ordered phase ($L2_1$-type) should form at a lower temperature. Since both $B2$-type and $L2_1$-type structures are related to the disordered body-centered cubic (bcc) structure ($A2$ type), [1999Ove] determined experimentally the chemical order transition $B2' \rightarrow L2_1$ and theoretically investigated the $A2 \rightarrow B2' \rightarrow L2_1$ -type ordering reaction* using the Bragg-Williams-Gorsky (BWG) model for the $Ga_{50-x}Mn_xNi_{50}$ alloys with $15 \leq x \leq 35$. Trial experiments with a $Ga_{25}Mn_{25}Ni_{50}$ alloy showed that the $L2_1$ ordering reaction cannot be arrested by quenching the alloy from high temperature. Hence, in situ neutron diffraction measurements and differential thermal analysis (DTA) of the $Ga_{50-x}Mn_xNi_{50}$ alloys were carried out by [1999Ove]. Arc melted alloys were prepared using very high purity

*This transformation sequence was used by [1996Cor].

Table 1 Phases of the Ga-Mn-Ni system and their structure data

Phase designation	Composition (a)	Pearson's symbol	Space group	Type	Lattice parameter, nm		
					a	*b*	*c*
γ	(Ni), (γMn), (γMn, Ni)	*cF*4	$Fm\bar{3}m$	Cu	...	...	...
α	(αMn)	*cI*58	$I\bar{4}\ 3m$	αMn	...	...	...
β	(βMn)	*cP*20	$P4_132$	βMn	...	...	...
δ	(δMn)	*cI*2	$Im\bar{3}m$	W	...	...	...
Ga	(Ga)	*oC*8	*Cmca*	α Ga	...	...	...
ε_1	$GaMn_{2.5}$	...	...	...	...	...	...
γ_2	$GaMn_{1.7}$ (HT)	*tI*8	*I*4/*mmm*	Al_3Ti	0.3901	...	0.7120
γ_3	$GaMn_{1.4}$ (55-63 Mn)	*tP*4	*P*4/*mmm*	AuCu	0.3898	...	0.3586
λ	$GaMn_{1.2}$ (HT) (39.5-55 Mn)	*hR*26	*R*3*m*	Cr_5Al_8	0.898 $\alpha = 88.3°$	...	...
η	$GaMn_{1.2}$ (LT) (40-50 Mn)	...	...	...	...	...	...
ι	$Ga_{2.3}Mn$	*tP*14	*P*4/*mbm*	...	0.8803	...	0.2694
ϕ	$Ga_{3.3}Mn$	*cI*10	*I*432	Hg_4Pt	0.5591	...	...
ω	$Ga_{4.6}Mn$	*oC*28	*Cmcm*	Al_6Mn	0.8974	0.8842	0.9940
β_1	$GaNi_3$	*cP*4	$Pm\bar{3}m$	$AuCu_3$	0.35850	...	...
δ'	Ga_3Ni_5	*oC*16	*Cmmm*	Ga_3Pt_5	0.376	...	0.339
ε	Ga_2Ni_3 (HT)	*hP*4	$P6_3/mmc$	AsNi	0.3995	...	0.498
γ'	Ga_2Ni_3 (LT)	...	...	...	1.3785 $\beta = 35.913°$	0.7883	0.8457
ν	GaNi	*cP*2	$Pm\bar{3}m$	CsCl	0.2873	...	...
θ	Ga_4Ni_3	*cI*112	*Ia*3*d*	Ga_4Ni_3	1.141	...	...
β_2	Ga_3Ni_2	*hP*6	*P*3*m*1	Al_3Ni_2	0.405	...	0.489
ρ	Ga_4Ni	*cI*52	$I\bar{4}3m$	Cu_5Zn_8	0.8406	...	...
γ_1	$MnNi_3$	*cP*4	$Pm\bar{3}m$	$AuCu_3$	0.3598	...	...
ς	$MnNi_2$ (HT)	...	...	...	...	...	...
ς'	$MnNi_2$ (LT)	...	...	...	...	...	...
ν	MnNi (HT)	*cP*2	$Pm\bar{3}m$	CsCl	0.29743	...	...
η_1	MnNi (MT)	*tP*4	*P*4/*mmm*	AuCu	0.37218	...	0.35295
η_2	MnNi (LT)	...	...	...	...	...	...
ξ	Mn_2Ni	...	...	...	...	...	...
κ	Mn_3Ni	...	...	...	...	...	...
ν'	$GaMnNi_2$	...	$Fm\bar{3}m$	$AlMnCu_2$	0.5825	...	...
ν' (M)	Martensite (b)	...	$P4/mmm$	AuCu	0.592	...	0.556
ν'' (M)	Martensite (c)	...	$I4/mmm$	Al_3Ti	0.418	...	0.556 (d)

(a) (HT), (MT), and (LT) represent high temperature, medium temperature, and low temperature, respectively. (b) From CsCl-type structure. (c) From $GaMnNi_2$ structure. (d) *c* parameter given here is *c*/2 of superstructure cell

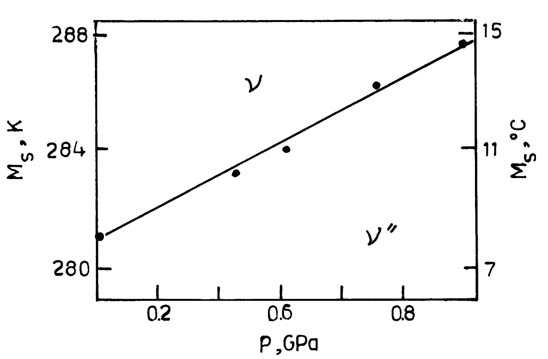

Fig. 4 Variation of M_s temperature of $GaMnNi_2$ single crystal as a function of hydrostatic pressure *P* [1996Che]

component elements. DTA traces were taken during heating and cooling of samples in the temperature range of 100-1000 °C. For in situ neutron diffraction, carried out using a water-cooled furnace going up to 1000 °C, the specimens were heated to 850 °C to disorder them and cooled to the required temperature, equilibrated for 1 h, and diffraction patterns were recorded. DTA traces indicated two thermal effects, the first one, a very small one, due to the $B2' \rightarrow L2$, transformation and the second one, a large one due to $B2' \rightarrow$ liquid transformation. The experimental results are given in Fig. 6. No $A2 \rightarrow B2'$ transformation could be detected by DTA. Neutron diffraction experiments indicated the evolution of $L2_1$-type structure as temperature was decreased. The intensity of diffraction peaks in the diffraction patterns were used to estimate the order parameters and

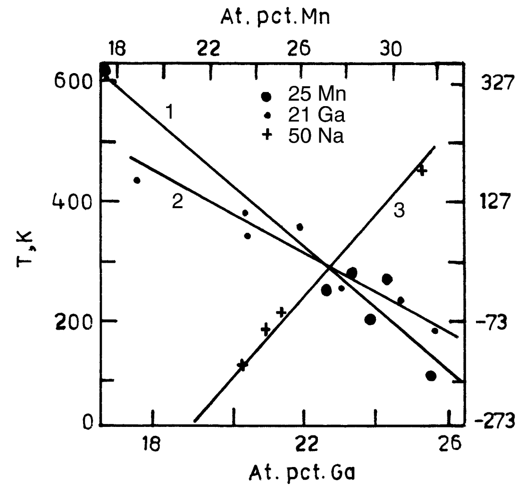

Fig. 5 Evolution of M_s temperature of Ga-Mn-Ni ν phase alloys as a function of Ga (1) and Mn (2) and (3) at approximately constant value of the third element [1995Che]

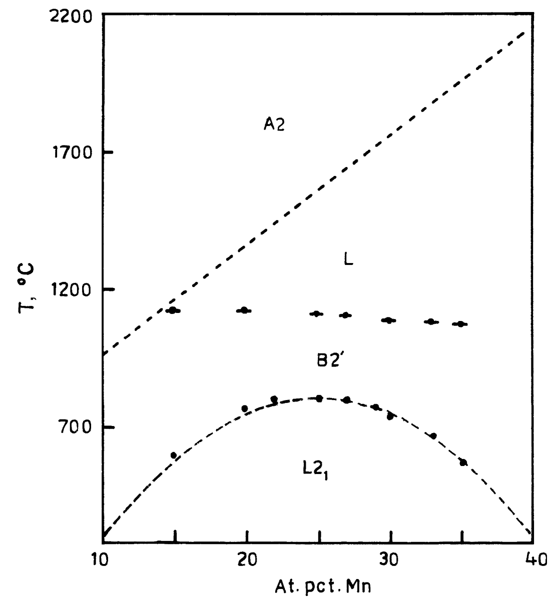

Fig. 6 Experimental and theoretical composition-temperature diagram for the GaNi-MnNi quasi-binary system. DTA data for $B2' \rightarrow L2_1$ transformation, melting temperatures of alloys, and the calculated phase boundary (dashed line) using BWG model [1999Ove]

used in the BWG model to estimate the theoretical $A2 \rightarrow B2'$ and $B2' \rightarrow L2_1$, transition temperatures as a function of composition. These transition temperatures are also indicated in Fig. 6. The results indicate that the alloys melt before the $A2 \rightarrow B2'$ transition temperature can be reached. For the $B2' \rightarrow L2_1$ transformation the experimental and theoretical data agree very well. The results indicate that a pseudobinary exists between the GaNi and the MnNi phases with a very flat liquidus temperature over the composition region investigated. Further work should be done at the two ends of the pseudobinary.

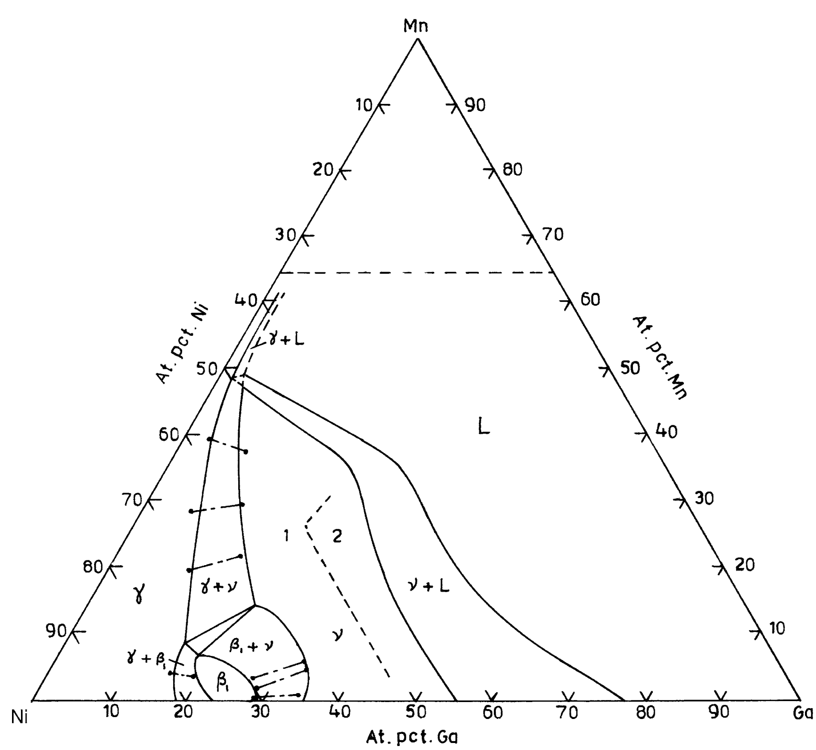

Fig. 7 A partial isothermal section of Ga-Mn-Ni system at 1000 *degr*C [2001Wed]. The alloys in the area 1 produces on quenching martensite of AuCu structure, whereas the alloys in the area 2 produces on quenching martensite with cell parameter *a* being same as AuCu-type structure but the *c* parameter is doubled

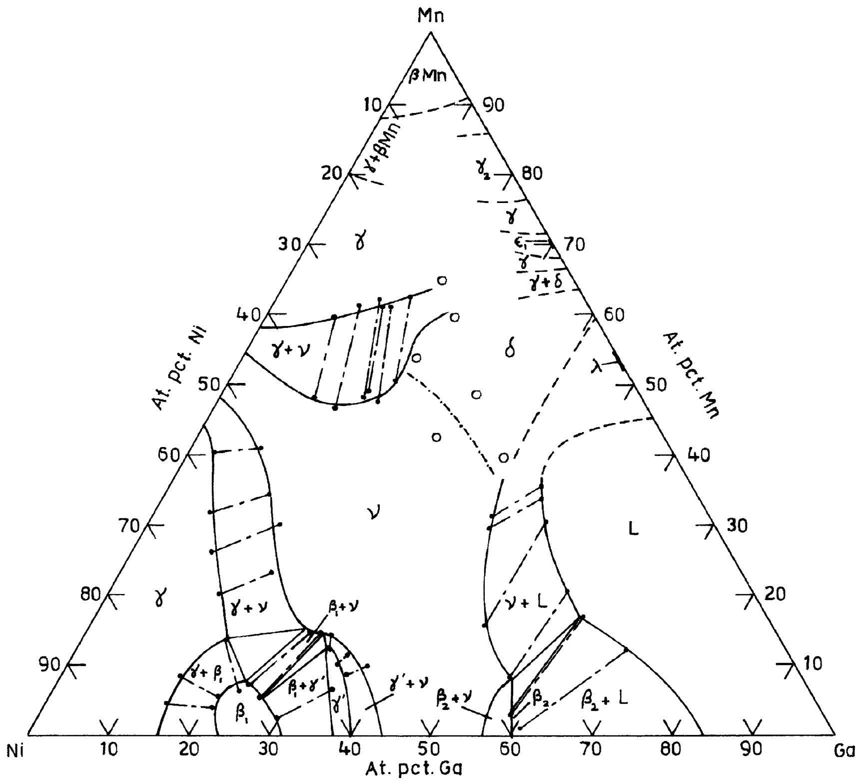

Fig. 8 A partial isothermal section of Ga-Mn-Ni system at 800 °C [2001Wed]. Dash-dot line indicates probable phase boundary between the ν and δ phases

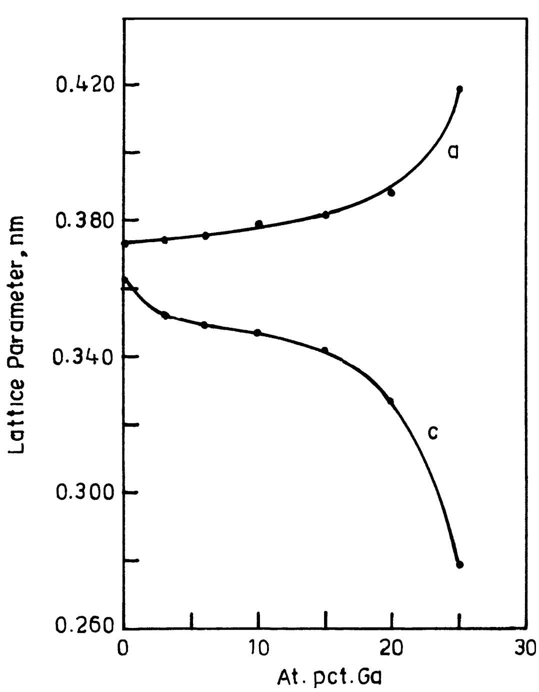

Fig. 9 Lattice parameter of martensite phase for $Ga_{50-x}Mn_xNi_{50}$ alloys with AuCu-type cell disregarding the doubled *c* axis of some of the alloys [2001Wed]

A more detailed investigation of the Ga-Mn-Ni system, up to ~65 at.% Mn, was done by [2001Wed]. The alloys were prepared by using 99.99 mass% Ga and Ni and 99.9 mass% Mn in MgO crucibles, vacuum sealed in silica tubes, and melted at 1200 °C for 2 h, furnace cooled to 1000 ° or 800 °C, kept at these temperatures for 5 h and quenched in ice water. Optical microscopy, x-ray diffraction, and x-ray spectrometry (EPMA) were used to characterize the alloys. A few diffusion couples were also used (heated to 1000 °C for 1 h followed by 7- to 10 days annealing at 1000 °C or 5 to 6 weeks annealing at 800 °C). The diffusion zones were analyzed by x-ray spectroscopy (EPMA). Two partial isothermal sections were established at 1000 °C (Fig. 7) and 800 °C (Fig. 8).

Figure 7 shows the partial isothermal section of Ga-Mn-Ni system at 1000 °C. The single-phase regions found in the isothermal section are the fcc γ phase extending from the Ni corner to 65 at.% Ni and possibly beyond, a small extension (~10 at.% Mn) of the $AuCu_3$-type β_1 phase and the CsCl-type ν phase was found to extend from the Ga-Ni system to almost the Mn-Ni system. The ν phase is CsCl-type at 1000 °C, but on quenching from high temperatures these alloys undergo martensitic transformation. The alloys in the composition region Ni >50 at.% on quenching give the AuCu-type martensitic phases. For the alloy compositions Ni $\leq$ 50 at.% and Mn<35 at.%, the alloys give the $L2_1$-type ordering and produce a martensite that is AuCu type but with doubled

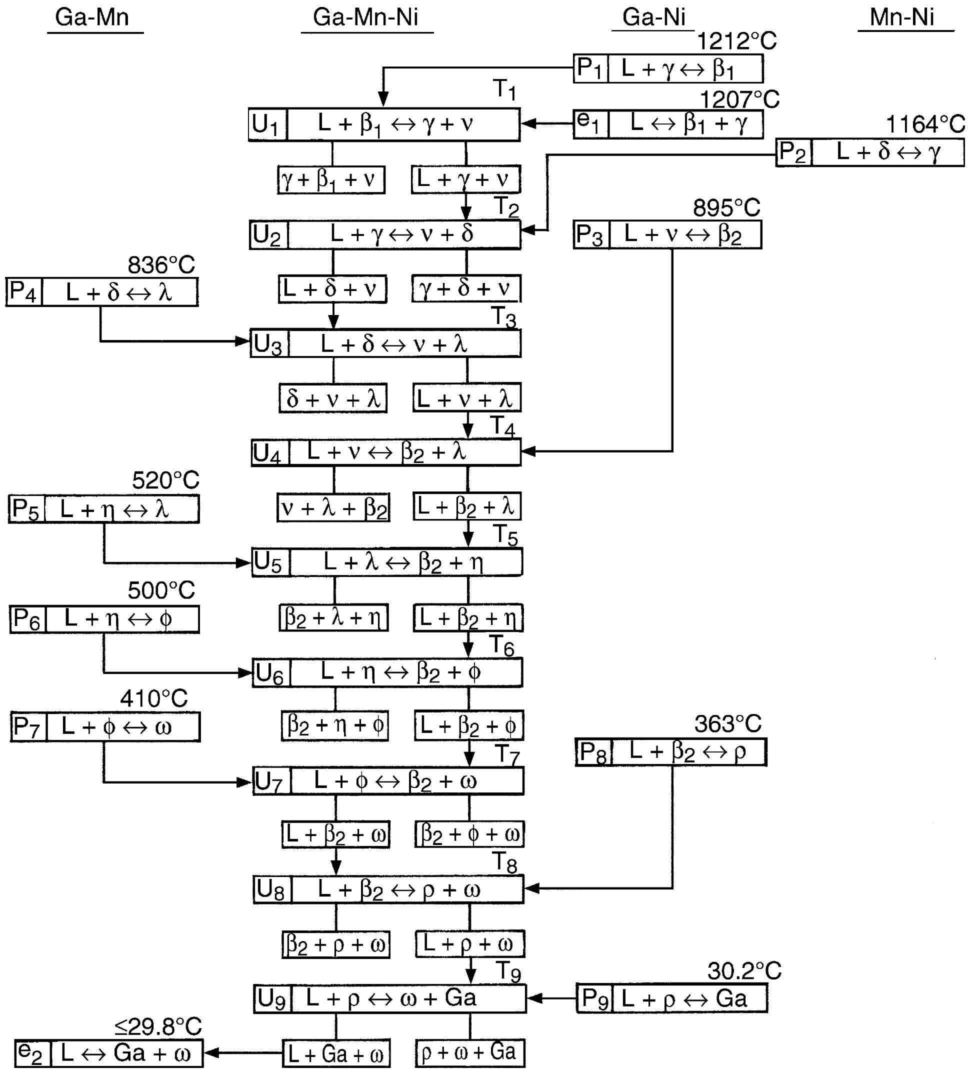

Fig. 10 Probable reaction scheme for the Ga-Mn-Ni system involving the liquid phase

c axis. Disregarding this difference between the two martensitic structures, the AuCu-type cell parameters of alloys with 50 at.% Ni are given in Fig. 9. At 800 °C (Fig. 8), the partial isothermal section shows extension of the ν phase from the Ga-Ni to the Mn-Ni binary, and additional phases observed are the γ' phase, the β_2 phase, and the δ phase, which is an extension of the (δMn) disordered bcc phase from the Ga-Mn binary. The transition region for the ν phase and the δ phase was not determined precisely. The phase boundaries close to the Ga-Mn binary were not determined by [2001Wed]. Since at 800 °C there are large numbers of phases that exist in the Ga-Mn system above 50 at.% Mn (the phases that exist in the Ga-Mn systems at 800 °C with Mn content >50 at.% are indicated in Fig. 8), the phase boundaries at the Ga-Mn system are incomplete and require further investigation. A probable βMn -phase region at the Mn corner is, however, indicated in Fig. 8.

The phase regions observed in the 1000 and 800 °C isothermal sections—that is, the three-phase regions $\gamma + \beta_1 + \nu$ and $\gamma + \beta_2 + L$ and the existence of a δ -phase region adjacent to the Ga-Mn binary line—can be used to suggest a probable reaction scheme involving the liquid phase (Fig. 10) and a liquidus projection (Fig. 11) for the Ga-Mn-Ni system. The binary reactions β_1 and e_1 at the Ga-Ni binary are expected to give a peritectic-type four-phase reaction $U_1 : \mathrm{L} + \beta_1 \leftrightarrow \gamma + \nu$ from which the three-phase equilibrium $\gamma + \beta_1 + \nu$ will be realized (Fig. 10), and the peritectic reaction p_3 at the Ga-Ni binary will give the $\mathrm{L} + \lambda + \beta_2$ three-phase equilibrium. Since the phase equilibria at the Ga-Mn side of the Ga-Mn-Ni system has not been well established, the rest of the proposed reaction

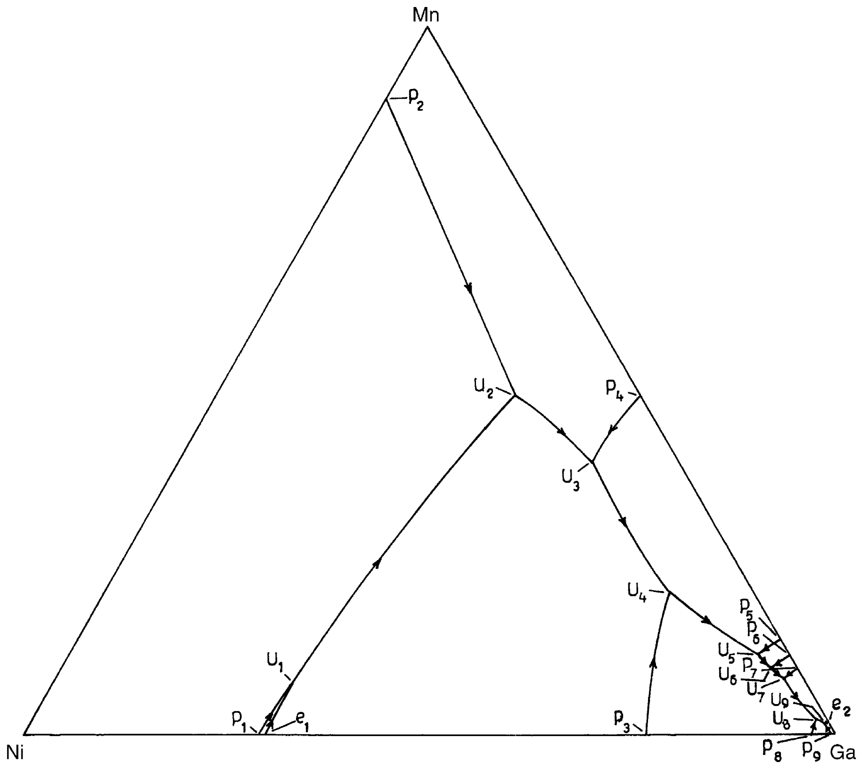

Fig. 11 Probable liquidus projection (schematic) for the Ga-Mn-Ni system

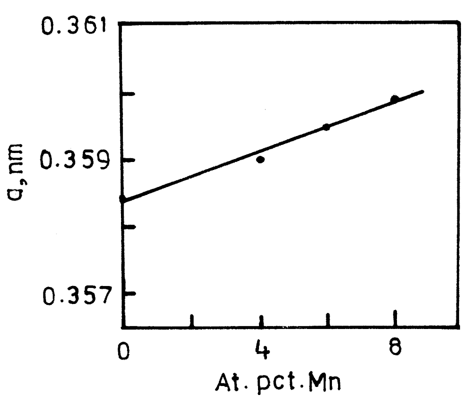

Fig. 12 Lattice parameter variation of $GaNi_3$ phase as a function of Mn content [1985Mis]

scheme and the liquidus projection cannot presently be further verified. More detailed investigation of the Ga-Mn-Ni system should be done at the high-Mn side of the ternary system, especially close to the Ga-Mn binary.

Mechanical properties of Ni-base superalloys are enhanced by dispersion of Ni_3Al phase alloyed with other elements; the enhancement of property occurs due to lattice misfit to increase coherency strain between the two phases. [1985Mis] made a systematic study of change in lattice parameters of Ni, Ni_3Al, and Ni_3Ga phases with addition of various third elements. Addition of Mn to Ni_3Ga was found to increase lattice parameter of the Ni_3Ga phase with increase in the Mn content (Fig. 12).

References

1960Ham: F.A. Hames, Ferromagnetic Alloy Phases Near the Compositions Ni_2MnIn, Ni_2MnGa, Co_2MnGa, Pd_2MnSb and PdMnSb, *J. Appl. Phys.*, 1960, **31**(5), p 3705-3715

1968Web: P.J. Webster and R.S. Tebble, *J. Appl. Phys.*, 1968, **39**, p 471 (quoted by [1984Web])

1984Web: P.J. Webster, K.R.A. Ziebeck, S.L. Town, and M.S. Peak, Magnetic Order and Phase Transformation in Ni_2MnGa, *Philos. Mag. B*, 1984, **49**(3), p 295-310 (Crys Structure)

1985Mis: Y. Mishima, S. Ochiai, and T. Suzuki, Lattice Parameters of Ni (γ), Ni_3Al (γ') and Ni_3Ga (γ') Solid Solutions with Additions of Transition and B-subgroup Elements, *Acta Metall.*, 1985, **33**(6), p 1161-1169

1990Zas: I.K. Zasimchuk, V.V. Kokorin, V.V. Martynov, A.V. Tkachenko, and V.A. Cherenenko, Crystal Structure of Martensite in Heusler Alloy Ni_2MnGa, *Phys. Met. Metall.*, 1990, **69**(6), p 104-108 (Phase Transformation)

1991Nas: P. Nash, *Phase Diagrams of Binary Nickel Alloys*, ASM International, 1991 (Review)

1995Che: V.A. Cherenenko, E. Cesari, V.V. Kokorin, and I.N. Vitenko, The Development of New Ferromagnetic Shape Memory Alloys in Ni-Mn-Ga System, *Scr. Met. Mater.*, 1995, **33**(8), p 1239-1244 (Physical Properties)

1996Che: V.A. Cherenenko and V.A. L'vov, Thermodynamics of Martensitic Transformation Affected by Hydrostatic Pressure, *Philos. Mag. A*, 1996, **73**(4), p 999-1008

1996Cor: R. McCormack and D. de Fontain, First Principles Study of Multiple Order-disorder Transitions in the Cd_2AgAu Heusler Alloys, *Phys. Rev. B*, 1996, **54**(14), p 9746-9755

1997Wir: S. Wirth, S. Leith-Jasper, A.N. Vasilev, and J.M.D. Coey, Structural and Magnetic Properties of Ni_2MnGa, *J. Magn. Magn. Mater.*, 1997, **167**, p L7-L11

1999Ove: R.W. Overholser, M. Wuttig, and D.D. Neumann, Chemical Ordering in Ni-Mn-Ga Heusler Alloys, *Scr. Mater.*, 1999, **40**(10), p 1095-1102 (Phase Equilibria, #)

1999Wed: B. Wedel, M. Suzuki, Y. Murakami, C. Wedel, J. Suzuki, D. Shindo, and K. Itagaki, Low Temperature Crystal Structure of Ni-Mn-Ga Alloys, *J. Alloys Compds.*, 1999, **290**, p 137-143 (Crys Structure)

2001Wed: C. Wedel and K. Itagaki, High Temperature Phase Relations in the Ternary Ga-Mn-Ni System, *J. Phase Equilibria*, 2001, **22**(3), p 324-330 (Phase Equilibria, #)

# indicates presence of phase diagram.

Ga-Mn-Ni evaluation contributed by **K.P. Gupta**, The Indian Institute of Metals, Metal House, Plot 13/4, Block AQ, Sector V, Calcutta, India. Literature searched through 1996. Dr. Gupta is the Alloy Phase Diagram Co-Category Program Editor for ternary nickel alloys.